[Frontiers in Bioscience, Landmark, 24, 798-818, March 1, 2019]

IFN-Alpha1 antisense RNA represses human influenza A virus growth in a guinea pig system

Ryou Sakamoto[1], Shiwen Jiang[1], Yusuke Tsukada[2], Hiroyuki Tsujimoto[2], Tominori Kimura[1]

[1]Laboratory of Microbiology and Cell Biology, Department of Pharmacy, College of Pharmaceutical Sciences, Ritsumeikan University, Kusatsu, Shiga, Japan, [2]Material Business Division, Hosokawa Micron Corporation, Hirakata, Osaka, Japan

TABLE OF CONTENTS

1. ABSTRACT

We reported a natural antisense (AS) long non-coding RNA as an important modulator of interferon-Alpha1 (*IFNA1*) mRNA levels. We showed that IFN-Alpha1 AS promotes *IFNA1* mRNA stability by transient duplex formation and inhibition of miR-1270-induced mRNA decay. Here, we performed a proof-of-concept experiment to verify that the AS-mRNA regulatory axis exerts *in vivo* control of innate immunity. We established a model system for influenza virus infection using guinea pig, which encodes a functional *MX1* gene for the type I IFN pathway. This system allowed us to investigate the effects of antisense oligoribonucleotides representing functional domains of guinea pig IFN-Alpha1 AS on gp*IFNA1* mRNA levels and, consequently, on viral proliferation in the respiratory tract of *influenza virus*-infected animals. We demonstrated that pulmonary-administered asORNs inhibited the proliferation of the virus in the animals by modulating *IFNA1* mRNA levels. These results indicate that, in light of the proposed actions, asORNs may modulate the level of *IFNA1* mRNA *in vivo*, indicating that IFN-Alpha1 AS plays a pivotal role in determining the outcome of type I IFN responses.

2. INTRODUCTION

During the last decade, high-throughput technologies, such as next generation

sequencing, have shown that the vast majority of a genome is transcribed, allowing the complexity of whole transcriptomes to be fully appreciated. As a result, an overwhelming number of long non-coding RNAs (lncRNAs) has been newly identified, leading to an increased understanding of the complexity of biological processes.

LncRNAs are defined as transcripts of more than 200 nucleotides that are not translated into proteins. They form a heterogeneous class of non-coding transcripts (1), which are subdivided in five categories based on their genomic localization: pRNAs (promoter-associated RNAs), eRNAs (enhancer-associated RNAs), gsRNAs (gene body-associated RNAs), lincRNAs (long intergenic or intervening non-coding RNAs) and NATs (Natural Antisense Transcripts) (for a review see (2) and REFERENCES therein).

It is thought that most lncRNAs originate within a 2 kb region surrounding the Transcription Start Site (TSS) of protein-coding genes (65% of lncRNAs overlap with a promoter, pRNAs), map to enhancer regions (19%; eRNAs), derive from antisense transcripts that overlap with annotated gene bodies (5%, NATs), or are associated with the bodies of protein-coding genes (gsRNA) (3, 4). The remaining lncRNAs (11%) originate from more distal (>2 kb) unannotated regions and are referred to as lincRNAs (5, 6).

Transcriptional regulatory elements, such as enhancers and promoters, can initiate transcription bi-directionally (7, 8); therefore, the majority of lncRNAs are initiated at promoters or enhancers. Many lncRNAs are localized in the nucleus (9), supporting the notion that lncRNAs are key regulators of epigenetic regulation. However, recent reports of local gene regulation by lncRNA loci suggest that in many cases, the act of transcription or DNA elements within the lncRNA locus are more likely to be a source of regulatory activity than the lncRNA itself (for a review see (10) and references therein), indicating more precise roles of lncRNAs as scaffolds for nuclear processes or guides for ribonucleoprotein complexes (2).

Another crucial role of lncRNAs has been highlighted in the field of post-transcriptional gene regulation (11, 12). For this function, lncRNAs leave the site of transcription and operate in *trans*. *Trans*-acting lncRNAs may function by modulating the activity or abundance of proteins or RNAs to which they bind (10). For example, the lncRNA, *NORAD* (noncoding RNA activated by DNA damage), functions as a molecular decoy for the RNA-binding proteins, PUMILIO1 (PUM1) and PUMILIO2 (PUM2) (13, 14), indicating that *NORAD* functions as a negative regulator of PUM1/PUM2 by limiting the availability of these proteins to interact with mRNA targets (10). Moreover, lncRNAs have the ability to regulate the abundance or activity of other RNAs to which they bind through base-paring interactions. These lncRNAs, termed competing endogenous RNAs or ceRNAs, have been suggested to broadly titrate microRNA (miR) availability (15).

A key feature of these lncRNAs is that they often require stoichiometric interaction with their target molecules to exert measureable regulatory effects. It is, therefore, interesting to note that these lncRNAs often form networks with ceRNA partners to fulfill the gap between the cellular copy numbers of the lncRNA and its target(s) (16) (for a review see also (17)).

Type I interferons (IFNs) and their downstream products collectively limit viral proliferation and spread; therefore, IFN-Alpha-based treatments are widely used for the treatment of chronic viral infections. A large number of IFN regulation studies have focused on IFN-Alpha protein function, particularly on the transcriptional activation of type I *IFN* genes and the IFN-Alpha signal transduction cascade. However, regulation at the RNA level has received less attention (18).

During our studies on a novel *cis*-acting element that is responsible for the

CRM1-dependent nuclear export of human IFN-Alpha1 (*IFNA1*) mRNA (19), we observed that deletion of a core structure in a stem-loop region formed by the element selectively impaired the stability of the *IFNA1* mRNA. This finding led us to identify IFN-Alpha1 antisense RNA (AS), a natural AS transcribed from the opposite strand of the *IFNA1* gene that acts as an important modulator of *IFNA1* mRNA levels by promoting *IFNA1* mRNA stability (18). This regulatory function was mediated in two ways; by transient duplex formation between IFN-Alpha1 AS and the mRNA, and by inhibiting miR-1270-induced mRNA decay through the shared miR-1270 response elements (MRE-1270s) between IFN-Alpha1 AS and mRNA (16, 18).

In the accompanying report (20) and our previous study (18), we identified guinea pig (*Cavia porcellus*) *IFNA1*, whose mRNA was expressed with IFN-Alpha1 AS in a concordant manner, indicating a concordant regulation in the expression of gpIFN-Alpha1 AS/mRNA, similar to the observations in *Sendai virus*-infected human Namalwa lymphocytes.

In the present study, we performed a proof-of-concept (POC) experiment to confirm that the NAT-mRNA regulatory network exerts control over innate immunity *in vivo*. For this, we established a unique model system in guinea pigs, which possess a functional *Mx* (Mx dynamin-like GTPase) gene (21). This enabled us to investigate the IFN response to influenza virus infection (22). We employed poly(D,L-lactide-co- glycolide) (PLGA) nanoparticles as a respiratory drug carrier (23, 24), which allowed us to deliver antisense oligoribonucleotides (asORNs) designed from the functional domains of guinea pig (gp)IFN-Alpha1 AS directly to the sites of virus infection. With this system, we verified that gpIFN-Alpha1 AS functional domains modulated the expression levels of gpIFN-Alpha1 AS/mRNA, resulting in inhibition of viral proliferation in the respiratory tract of influenza A virus-infected animals.

3. MATERIALS AND METHODS

3.1. Reagents

PLGA (lactide:glycolide = 75:25, MW = 20,000) and polyvinylalcohol (PVA; Gohsenol EG05) were purchased from Wako Pure Chemical Industries (Osaka, Japan) and Nippon Synthetic Chemical Industry Co. (Tokyo, Japan), respectively. Chitosan (GH-400EF) was obtained from NOF Corporation (Tokyo, Japan). All other chemicals were obtained commercially and were of analytical grade.

3.2. Cell culture and virus propagation

Gp104C1 cells (fetal fibroblasts; ATCC CRL-1405) and MDCK (Madin-Darby canine kidney) cells (ATCC CCL-34) were maintained as previously described (18) (see also the accompanying report (20)).

The rodent-adapted PR/8 virus, *influenza virus* A/Puerto Rico/8/34 (A/PR/8/34, H1N1) (25) was propagated in the allantoic cavity of 10-day-old embryonated hen eggs as previously described (18). The viral titers were measured with a plaque-forming assay using MDCK cells.

3.3. Transfection

To silence the expression of gpIFN-Alpha1 AS, 2.9 μg, (an amount previously optimized for both human and guinea pig cells (18)), of each phosphorothioate-modified sense oligodeoxynucleotide (seODN) (Eurofins genomics, Tokyo, Japan) was added to 104C1 cells and magnet-assisted transfection (MATra; IBA, Goettingen, Germany) was performed as described previously (18). pSV-Beta-galactosidase control vector (Promega, Madison, WI, USA) (0.1 μg) was included in each transfection mixture to normalize transfection efficiencies. After incubation for 6 h at 37°C, transfected cells were infected with the PR/8 virus at a multiplicity of infection of 25.5 as previously described (18). After further incubation at 37°C for 0-48 h, infected cells were harvested to examine gp*IFNA1* mRNA/AS as described below or to measure

Table 1. Antisense oligoribonucleotides employed to over-express the functional domain of gpIFN-Alpha1 AS

Name	Location	Sequence[1]
asORN3	*cpIFNA1* nt 270-252	G(M*)A(M*)G(M*)G(M*)U(M*)U(M*)G(M*)A(M*)A(M*)G(M*)G(M*)U(M)C(M*)U(M*)G(M*)C(M*)C(M*)U(M*)G(M*)-
asORN4	*cpIFNA1* nt 288-270	U(M*)G(M*)A(M*)G(M*)U(M*)C(M*)C(M*)U(M*)C(M*)U(M*)G(M*)A(M*)U(M*)C(M*)U(M*)G(M*)A(M*)A(M*)G(M*)-
ncasORN	negative control	C(M*)U(M*)C(M*)C(M*)A(M*)A(M*)C(M*)U(M*)U(M*)C(M*)C(M*)A(M*)G(M*)A(M*)C(M*) G(M*)G(M*)A(M*)C(M*)-
[1]An M indicates 2′-*O*-methylation and an asterisk indicates a phosphorothioate bond		

Table 2. Primers used for silencing guinea pig IFN-Alpha1 AS[1]

Name	Sequence[1]	Nucleotide number of *IFNA1* of *C. porcellus*
seODN2	C*T*T*CCATGAGATGACCA*G*G*C	237-256
seODN3	C*A*G*GCAGACCTTCAAC*C*T*C	252-270
seODN4	C*T*T*CAGATCAGAGGAC*T*C*A	270-288
seODN5	G*A*G*GACTCATCTGCTG*C*C*T	280-298
seODN6	C*T*G*CCTGGAACCAGAG*T*C*T	293-311
[1]An asterisk indicates a phosphorothioate bond		

Beta-galactosidase activities according to the manufacturer's instructions (Beta-Glo assay system; Promega). The expression levels of *IFNA1* mRNA/AS steadily increased in both Namalwa lymphocytes and 104C1 cells for the first 24 h after viral infections (18); therefore, 104C1 cells were collected for RNA analysis at 0, 24, 36 and 48 h after viral infection. For the Beta-galactosidase analysis, the cells were collected at 48 h after virus infection. The seODNs were designed according to the gp*IFNA1* mRNA sequence and included loops that might cross-hybridize with the loops of the IFN-Alpha1 AS, as previously described (18). The names and sequences of seODNs are listed in Table 2.

asORNs (Gene-Design, Osaka, Japan) were employed to introduce the functional domain-bearing fragment of gpIFN-Alpha1 AS into 104C1 cells as described above or into PR/8 virus-infected guinea pigs airways as described below. RNA samples were collected for subsequent RT-qPCR analysis as described above. The asORNs were designed to avoid Toll-like receptor (TLR)7/8-mediated immune effects by excluding the GU-rich motifs (26) and contained 2′-*O*- methylation modifications at each nucleotide position (27).

Their sequences and names are as follows (an M indicates 2′-*O*-methylation and an asterisk indicates a phosphorothioate bond) (Table 1).

3.4. Isolation of total cellular RNA and strand-specific reverse-transcription quantitative PCR (RT-qPCR) analysis

Total RNA was isolated from 104C1 cells as described previously (18) or from airway organs as described below. Strand-specific RT-qPCR was performed essentially as described previously (18). The copy numbers of gp*IFNA1* mRNA/AS were normalized to gpBeta-actin mRNA and determined by the regression lines from a set of standards as described previously (18). The names and sequences employed for the analysis were essentially the same as those described previously (18).

3.5. Preparation of asORN-containing PLGA nanoparticles (PLGA-asORN) and transfection of PLGA-asORN

PLGA-asORN were prepared by the emulsion solvent diffusion method in water as described previously (28). Briefly, PLGA was dissolved in an acetone/ethanol mixture and asORN3 or ncasORN solution was added to the PLGA solution. The resulting organic solutions were poured into an aqueous PVA solution containing chitosan and moderately stirred using a propeller-type agitator. The mixtures were agitated under reduced pressure to evaporate organic solvent, and asORN3 or ncasORN solution was further added to the resulting PLGA-asORN suspension to create PLGA-asORN3 and PLGA–ncasORN, respectively, before freeze-drying.

For PLGA-asORN transfection, 3 or 6 μg of asORN3 or ncasORN, contained in PLGA nanoparticles at the various percentages ranging from 1.46 - 2.26% (w/w), were resuspended in RNase-free water, vortexed, and sonicated at 4°C. The PLGA-asORNs were then added to 104C1 cells, which were then incubated in RPMI-1640 medium without fetal calf serum (FCS) for 4 hours. The culture medium was then diluted twice with 2 × concentrated RPMI-1640 containing 20% FCS, and the transfected cells were incubated at 37°C for an additional 2 hours prior to PR/8 virus infection.

3.6. Animals and PR/8 virus infection

Hartley guinea pigs (female, 4-weeks-old) were purchased from Shimizu Laboratory Supplies (Kyoto, Japan). During challenge studies, animals were housed in the animal facility at the Research Center for Animal Life Science, Shiga University of Medical Science (Shiga, Japan) according to an Institutional Care and Use Committee-approved protocol. Groups of four guinea pigs were anesthetized by intraperitoneal injection of pentobarbital sodium salt (30 mg/kg body weight) (Kyoritsu Seiyaku Corporation, Tokyo, Japan). They were subsequently inoculated intranasally with a non-lethal dose (10^6 plaque forming units (pfu)) of PR/8 virus (29) by instillation of 100 μl diluted virus into one nostril. For evaluation of PLGA-asORN3 effects on PR/8 virus proliferation, guinea pigs were pretreated with 100 μl PLGA-asORN3 or -ncasORN suspension (3% w/v) as described above at 6 h prior to the PR/8 virus infection. Some animals were given another inoculation of PLGA-asORN3 suspension at 18 h after the virus infection. Nasal and tracheal washes were collected from the anesthetized animals at various intervals after virus infection to assess the effects of PLGA-asORN3 on the PR/8 virus proliferation profile in the upper and lower respiratory pathways. The guinea pigs were monitored at the same intervals for changes in weight and rectal temperature to assess PLGA nanoparticle-induced morbidity. To determine the effects of PLGA-asORN3 on *gpIFNA1* mRNA/AS expression levels, animals were humanely euthanized by intraperitoneal injection of pentobarbital sodium salt (200 mg/kg of body weight) and the larynx and trachea tissues were harvested for strand-specific RT-qPCR RNA analyses.

3.7. Statistical analysis

Results in the Figures are representative of at least three independent experiments with triplicate samples generating similar findings. Differences presented in the Figures were analyzed using Student's *t* test.

3.8. Accession numbers

The genes employed in this study have the following accession numbers: AB671739 (*Cavia porcellus IFNA1*) and AF508792 (*Cavia porcellus ACTB*).

4. RESULTS

We previously reported that IFN-Alpha1 AS, a natural antisense RNA, is involved in determining post-transcriptional *IFNA1* expression (18). IFN-Alpha1 AS rapidly and reversibly upregulates *IFNA1* mRNA levels upon infection of human Namalwa B lymphocytes with *Sendai virus* and following infection of guinea pig 104C1 cells with PR/8 virus. The cytoplasmic sense-antisense interaction between the complementary transcripts resulted in stabilization of *IFNA1* mRNA. Alternatively, IFN-Alpha1 AS functions as a ceRNA to prevent

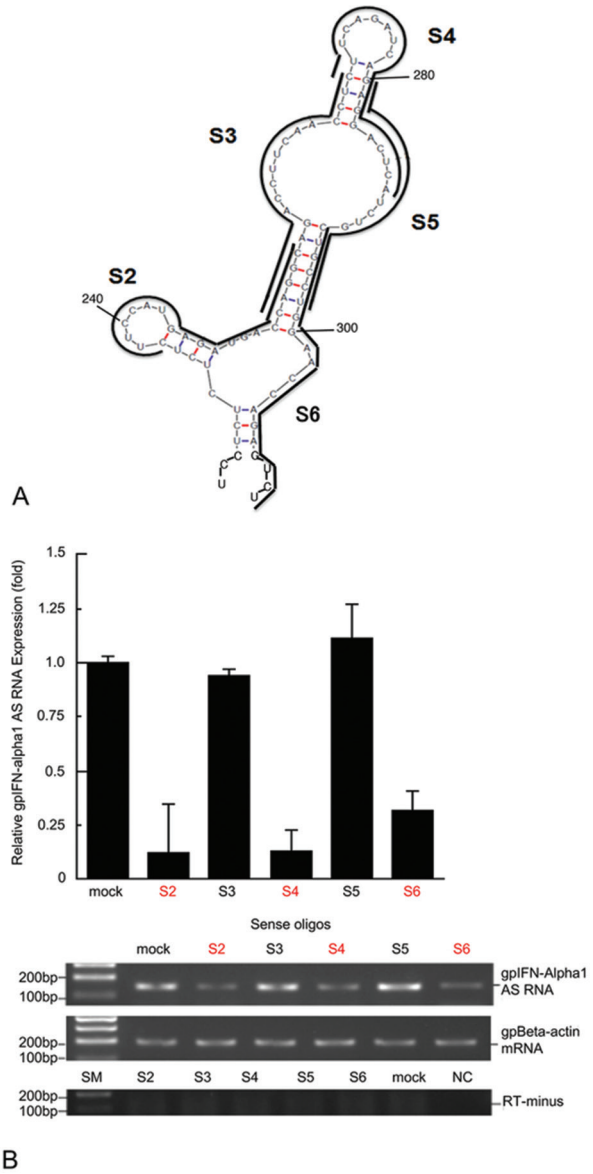

Figure 1. Silencing of gpIFN-Alpha1 AS by seODNs. (A) Location of seODNs S2-6 (black bold lines) are depicted along the common stem-loop structure present in the ten most predicted secondary structures of the gp*IFNA1* mRNA. (B) The effects of S2-6 on the constitutive expression levels of gpIFN-Alpha1 AS RNA were examined by strand-specific RT-PCR (top) and agarose gel electrophoresis (bottom). gpBeta-actin mRNA indicates an internal RNA standard. Values of three independent experiments are presented as the mean ± s.e.m. of three or four samples. Mock denotes mock-transfected. RT-minus shows no contamination of genomic DNA in the total cellular RNA samples examined.

miR-1270 from acting on *IFNA1* mRNA (16). These regulatory mechanisms play a pivotal role in determining the biological outcomes of type I IFN responses and whether or not pathogens are cleared effectively.

In the accompanying report (20), we confirmed identification of gp*IFNA1* and characterized its anti-viral function against PR/8 virus or EMCV infection. These results enabled us to investigate the *in vivo* IFN response

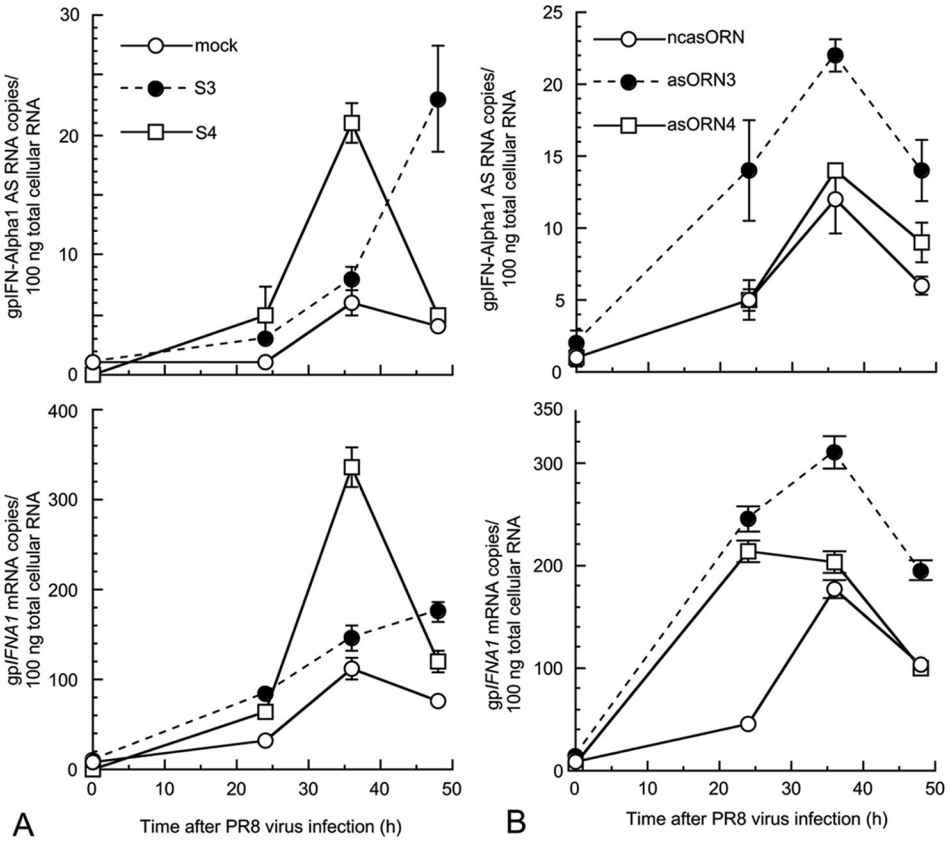

Figure 2. (A) Effect of silencing gpIFN-Alpha1 AS RNA on gp*IFNA1* mRNA expression. S3 (filled circle with broken line), S4 (open box with bold line) seODNs- or mock (open circle with bold line)-transfected 104C1 cells were subjected to PR/8 virus infection as described in the Materials and methods (S3, S4 and mock, respectively). RNA samples were collected at the indicated time points after viral infection and the copy numbers of gpIFN-Alpha1 AS RNA (top) and gp*IFNA1* mRNA (bottom) were determined. The results are presented as "Number of gpIFN-Alpha1 AS RNA or mRNA copies/100 ng of total cellular RNA" ± s.e.m. of three or four samples. Representative values of three independent experiments are presented. Error bars cannot be seen if they are smaller than the graph symbols. (B) Effect of asORNs on gpIFN-Alpha1 AS RNA and gp*IFNA1* mRNA expression levels. asORN3 (filled circle with broken line), asORN4 (open box with bold line)- or ncasORN (open circle with bold line)-transfected 104C1 cells were subjected to PR/8 virus infection as described in the legend to (A) (asORN3, 4 and ncasORN, respectively). RNA samples were collected at the indicated time points after viral infection and the copy numbers of gpIFN-Alpha1 AS RNA (top) and gp*IFNA1* mRNA (bottom) were determined as described in the legend to (A). The results are presented as "Number of gpIFN-Alpha1 AS RNA or mRNA copies/100 ng of total cellular RNA" ± s.e.m. of three or four samples. Representative values of three independent experiments are presented. Error bars cannot be seen if they are smaller than the graph symbols.

against viral infection by employing the guinea pig as a model animal. In the present study, we performed a POC experiment to confirm that the NAT-mRNA regulatory axis exerts control over innate immunity *in vivo*.

4.1. Effects of silencing constitutive gpIFN-Alpha1 AS on gp*IFNA1* mRNA expression

To explore this concept and to provide a possible platform for therapeutic intervention, we first planned to determine the functional domains of gpIFN-Alpha1 AS that are required for stabilizing gp*IFNA1* mRNA.

We therefore employed the seODN-mapping strategy (18) to analyze changes in mRNA levels after silencing gpIFN-Alpha1 AS expression. This silencing strategy is based on the sequence-specific binding of a seODN to the target AS RNA. The formation of an RNA-DNA hybrid then leads to destruction of the AS RNA by RNase H (18), indicating the functional

domains of gpIFN-Alpha1 AS that recognize gp*IFNA1* mRNA and that are necessary for stabilizing the mRNA (18). These data informed the POC experiment using the guinea pig model.

An RNA folding study by energy minimization using nearest neighbor energy parameters (30), indicated that most of the ten most likely theoretical secondary structures of gp*IFNA1* mRNA (data not shown) possess a common local domain structure (Figure 1A). We therefore designed seODNs, S2 to S6, whose sequences were taken from the single-stranded 'bubble' or 'loop' region of the common structure (Figure 1A). The seODNs were then tested for their ability to destroy endogenous gpIFN-Alpha1 AS. We did not include a negative control seODN at this stage, which could be designed from the double-stranded region of the common structure. We learned from the previous study (18) that not all seODNs designed from the single-stranded regions could recognize gpIFN-Alpha1 AS, and can therefore be employed as a negative control seODN.

As shown in Figure 1B, S2, S4 and S6 seODNs silenced the constitutive expression of gpIFN-Alpha1 AS, while S3 and S5 failed to silence the AS RNA (Figure 1B, compare S3 and S5 with mock). The silencing effects by S2, 4, and 6 were specific because gpBeta-actin mRNA levels were unaffected. We thus selected S4 to examine the effects of silencing gpIFN-Alpha1 AS on gp*IFNA1* mRNA levels. S3 seODN was employed as a tentative negative control for gpIFN-Alpha1 AS silencing.

104C1 cells were then transfected with either S4 or S3. As expected, S4-transfected cells had reduced gpIFN-Alpha1 AS expression at time 0; i.e. S4 reduced the constitutive expression levels of gpIFN-Alpha1 AS (Figure 2A top, compare S4 with S3 or mock gpIFN-Alpha1 AS copy number at 0 h) but neither S3-transfected nor mock-transfected cells showed this effect. Following PR/8 virus infection, expression was restored, reaching maximal levels 36 h after infection with approximately 4-fold higher expression in S4 cells than in S3 or mock cells. While mock cells then largely maintained gpIFN-Alpha1 AS expression levels, S4 cells showed a rapid reduction in AS copy numbers, of 76% at 48 h after PR/8 virus infection. These expression profiles of gpIFN-Alpha1 AS in 104C1 cells were very similar to that of human IFN-Alpha1 AS when its constitutive expression was silenced by a seODN and the transfected Namalwa cells were infected with SeV (18). The S3 seODN, however, unexpectedly increased gpIFN-Alpha1 AS copy number by approximately 3-fold, 48 h after PR/8 virus infection compared with at 36 h.

The time-course of gp*IFNA1* mRNA expression in S4-, S3- and mock-transfected cells was very similar to that of AS RNA (Figure 2A, bottom). While mock cells largely maintained similar mRNA copy numbers after reaching a maximal level at 36 h after virus infection, S4 cells rapidly reduced the expression of *IFNA1* mRNA from the peak level at 36 h, by 64% at 48 h after PR/8 virus infection. However, as observed for gpIFN-Alpha1 AS expression, S3 also increased gp*IFNA1* mRNA expression by 20% at 48 h after infection.

Neither S4 nor S3 seODNs encompass nonmethylated CpG motifs, the ligand recognized by TLR9 (26, 31), and no increase in *gpIFNA1* mRNA levels was observed in S4- or S3-transfected cells at time 0 after infection; i.e. at 6 h after transfection (Figure 1A bottom, compare S4 or S3 with mock). The subsequent increase in expression levels of gp*IFNA1* mRNA in the transfected cells precluded the possibility that S4 or S3 induced the gpIFN response by activation of TLR9 but that the response was caused following PR/8 virus infection.

4.2. Effect of over-expression of seODN-complementary asORNs on gpIFNA1 mRNA levels

The above results indicated that by analogy with silencing human IFN-Alpha1 AS (18), the S4 seODN could represent a recognition site of gpIFN-Alpha1 AS in the mRNA. We, therefore, further investigated gpIFN-Alpha1 AS function on mRNA expression, by over-expressing the mRNA

recognition site of gpIFN-Alpha1 AS. We designed antisense 2′-*O*-methyl oligoribonucleotide 4 (asORN4) with phosphorothioate bonds from the nucleotide sequence of S4 seODN. AsORN3 was also designed and included in the over-expression experiment because S3 showed a positive effect on gp*IFNA1* mRNA expression at the later stage of the silencing experiment.

As a negative control for the experiment, the nucleotide sequence of S3 seODN (gp*IFNA1*, nt 252 to 270) was reversed to create ncasORN (see Figure 1A). The following BLAT search (http://smithlabdb.usc.edu/cgi-bin/hgBlat?command) of ncasORN showed no off-targets present in the guinea pig genome (data not shown). AsORN4/3, ncasORN and seODNs were designed to exclude GU-rich motifs (26) to avoid TLR7/8-mediated IFN-Alpha and TNF-Alpha production.

104C1 cells were then transfected with asORNs or ncasORN. Six hours after transfection, cells were infected with PR/8 virus and subjected to analysis by strand-specific RT-qPCR. AsORN4 cells showed that gp*IFNA1* mRNA levels reached 4.7-fold higher levels compared with those expressed in ncasORN cells at 24 h after PR/8 virus infection (Figure 2B, bottom). As expected from the previous experiments investigating the asORN effects on human *IFNA1* mRNA levels in Namalwa B lymphocytes (18), asORN4 transfection did not change the levels of gpIFN-Alpha1 AS compared with those in ncasORN-transfected cells (Figure 2B, top). Neither asORNs nor ncasORN had any effect on gpBeta-actin expression (data not shown).

In contrast, asORN3 exerted unexpected effects on both gpIFN-Alpha1 AS and gp*IFNA1* mRNA expression levels. After transfection of asORN3, gpIFN-Alpha1 AS maintained higher expression levels throughout the experiment compared with those induced by asORN4, reaching maximal levels 36 h after infection with approximately 1.7-fold higher expression compared with asORN4 or ncasORN cells (Figure 2B, top).

asORN3 and asORN4 produced similar expression levels of gp*IFNA1* mRNA at 24 h after viral infection, but the mRNA levels were further raised by asORN3, reaching maximal levels 36 h after virus infection, similar to gpIFN-Alpha1 AS attaining the maximal level at the same time point. The highest expression levels of gp*IFNA1* mRNA in asORN3 cells were approximately 65% higher than those in asORN4 cells (Figure 2B, bottom).

The increase of gp*IFNA1* mRNA levels was not caused by aberrant RIG-I (retinoic acid-inducible gene-I) recognition of the asORNs, which are chemically synthesized 5′OH ssRNAs, or 5′OH dsRNAs formed between asORN4 or asORN3 and recognition sites of gpIFN-Alpha1 AS in the mRNA, because these molecules lack the 5′ triphosphate structure, a hallmark of viral RNAs and a prerequisite for RIG-I recognition (18, 32, 33).

The expression levels of both gpIFN-Alpha1 AS and gp*IFNA1* mRNA were higher in asORN3-transfected cells than in asORN4-transfected cells; therefore, asORN3 was selected for the following POC experiments using the guinea pig as the animal model.

4.3. Preparatory transfection of 104C1 cells with PLGA-asORN3

To investigate whether the *in vitro* effects of asORN3 on the levels of gpIFN-Alpha1 AS/mRNA expression similarly modulate the AS and mRNA levels *in vivo*, thereby, inhibiting PR/8 virus proliferation in the guinea pig model, we selected the PLGA nanoparticle, a biodegradable polymeric nanoparticle (34) (uptake of 400 nm diameter PLGA by A549 cells: V_{max} and K_m values were 39.8.4 µg/mg cell protein and 44 µg/ml, respectively (23)), as a drug carrier for pulmonary administration of asORN (23).

PLGA was successfully employed to transfect pig arteries *in vivo* with plasmid DNAs (35) and to deliver miRNA mimics in a biomaterial implant model (36). Importantly, the expression of inflammatory and IFN response markers was not increased by PLGA (37).

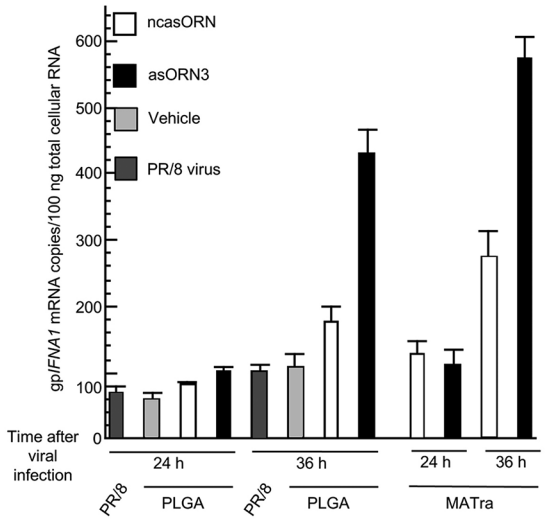

Figure 3. Preparatory experiments to optimize PLGA-dependent transfection efficiency in 104C1 cells. 104C1 cells were transfected with asORN3 (filled bar), ncasORN (open bar) or vehicle control (PLGA alone; light grey bar) by the PLGA or MATra methods, and the transfected cells were subjected to PR/8 virus infection, as described in the Materials and methods. Cells receiving the virus infection alone are indicated by dark grey bars. Transfections with 2.9 µg asORN3 or ncasORN as well as 0.1 µg pSV-Beta-galactosidase control vector were performed. RNA samples were collected at 24 or 36 h after viral infection and the copy numbers of *gpIFNA1* mRNA were determined as described in the Materials and methods. The results are presented as "*gpIFNA1* mRNA copies/100 ng of total cellular RNA" ± s.e.m. of three or four samples. Representative values of three independent experiments are presented.

Prior to the *in vivo* experiments, we conducted a series of preparatory transfection experiments using various lots of PLGA-asORN3 with PR/8 virus-infected 104C1 cells. PLGA nanoparticles with various surface charges (indicated by zeta-potential) and particle sizes (diameter) were synthesized to contain a range of asORN3 contents. They were then tested to optimize the amount of asORN3 and the time for transfection to maximize the expression levels of gpIFN-Alpha1 AS/mRNA.

Our previous experiments (22, 27) showed that decreasing the diameter to submicron levels and positive zeta potentials based on the chitosan-dependent protonation of the PLGA amino group increased the cellular uptake of PLGA nanoparticles; therefore, the initial experiment was performed using PLGA-asORN3 with a mean diameter of 157 nm and a zeta potential of +41 mV.

104C1 cells were transfected with 3 µg asORN3 by either the PLGA-asORN3 (1.3 w/w %) or the MATra method (see Materials and methods for the transfection control). The expression levels of gp*IFNA1* mRNA were then compared between the two methods. As expected from the results shown in Figure 2B, PLGA-asORN3 reproduced a time-dependent increase of gp*IFNA1* mRNA levels (Figure 3). The mRNA levels in PLGA-asORN3 cells were approximately 4-fold higher at 36 h after PR/8 virus infection compared with those observed in cells receiving virus infection alone or empty PLGA-transfection followed by virus infection (Figure 3, PR/8 virus and Vehicle).

In contrast, the PLGA-ncasORN cells at the same time point showed approximately 70% higher levels of gp*IFNA1* mRNA expression compared with those shown by the control cells, which were considerably lower (approximately 60%) than the levels expressed in the PLGA-asORN3 cells. However, the transfection efficiencies of PLGA-asORN3 were still lower than those obtained by the MATra method (Figure 3, compare filled bars at 36 h between PLGA and MATra).

To surpass the levels of gpIFN-Alpha1 AS/mRNA expressed by the MATra method, we tested the following two lots of PLGA-asORN3; lot A: 78 nm, +30 mV and 1.46 w/w % and lot B: 108 nm, +38 mV and 2.10 w/w %. The corresponding PLGA-ncasORN had mean diameters of 87 or 85 nm, zeta potentials of +28 mV each and 1.48 or 2.26 w/w % contents, respectively.

As shown in Figure 4, when 3 µg of asORN3 was transfected using lot A, PLGA-asORN3 generated 150% and 163% higher levels of gpIFN-Alpha1 AS and mRNA, respectively, compared with those obtained by the MATra method. In contrast, the corresponding PLGA-ncasORN showed approximately 46% lower levels of

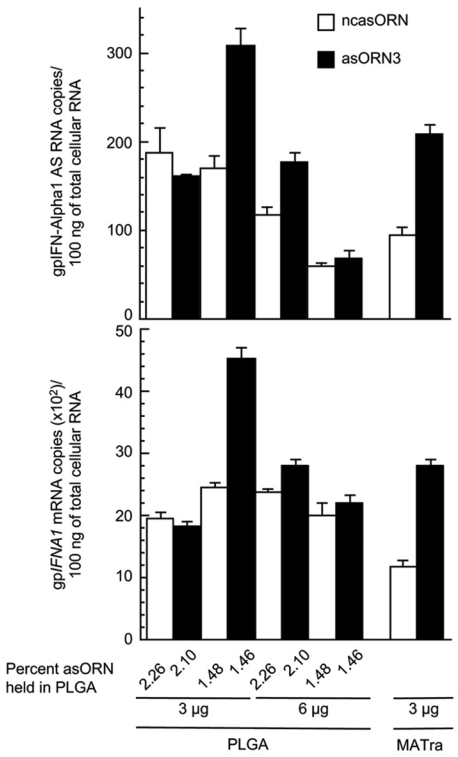

Figure 4. Optimization of PLGA-dependent transfection efficiencies of asORN3 to maximize gpIFN-Alpha1 AS RNA/mRNA expression levels in 104C1 cells. 104C1 cells were transfected with asORN3 (filled bar) or ncasORN (open bar) by the PLGA or MATra method, and the transfected cells were subjected to PR/8 virus infection, as described in the legend to Figure 2A. For PLGA-dependent transfection, 3 or 6 µg asORN3 or ncasORN, contained at various percentages (w/w) in PLGA nanoparticles (as described below the x axis of the figure) were employed, whereas 3 µg was used for MATra-associated transfection. RNA samples were collected at 36 h after viral infection and the copy numbers of gpIFN-Alpha1 AS RNA (top) and gp*IFNA1* mRNA (bottom) were determined as described in the legend to Figure 2A. The results are presented as "Number of gpIFN-Alpha1 AS RNA or mRNA copies/100 ng of total cellular RNA" ± s.e.m. of three or four samples. Representative values of three independent experiments are presented. According to the manufacturer's instructions, the amount of nucleotides for MATra-transfection was limited to 3 µg.

gpIFN-Alpha1 AS and mRNA compared with PLGA-asORN3. Six micrograms of lot A and both 3 and 6 µg of lot B did not surpass the expression levels of gpIFN-Alpha1 AS and mRNA by MATra. Based on these results, we concluded that PLGA-asORN3 of 78 nm, +30 mV and 1.46 w/w% and PLGA-ncasORN of 87 nm, +28 mV and 1.48 w/w% were applicable for the following *in vivo* POC experiment.

4.4. Dose-dependent reduction of PR/8 virus titers in guinea pigs following treatment with PLGA-asORN3

To investigate whether asORN3 raises gpIFN-Alpha1 AS and mRNA levels in the larynx and trachea tissues of influenza virus-infected guinea pigs, thereby inhibiting viral proliferation, guinea pigs received a single inoculation of PLGA-asORN3 (3 µg of asORN3) (Figure 5A, PLGA-asORN3/1). After 6 h the guinea pigs were challenged with a non-lethal dose of PR/8 virus (10^6 pfu/animal). Half of the guinea pigs received an additional 3 µg of asORN3 18 h after the virus infection (Figure 5A, PLGA-asORN3/1+1).

As expected from the *in vitro* data (Figure 2B), quantification of gpIFN-Alpha1 AS showed that the nasal administration of asORN3 increased the basal level of AS RNA expressed in both the upper and lower respiratory tracts. While the following viral challenge increased the gpIFN-Alpha1 AS expression in both the asORN3- and ncasORN-treated animals, the AS RNA levels in the asORN3-treated animals were 2.0-fold to 4.9-fold higher between time points 24 and 48 h post-PR/8 virus infection compared with those observed in the negative control, ncasORN-treated animals (Figure 5A top, PLGA-asORN3/1 and PLGA-ncasORN). The additional inoculation of asORN3 at 18 h post-infection further increased the AS RNA levels 3.6-fold to 6.1-fold at the same time points (24 – 48 h) post-infection compared with those obtained by ncasORN (Figure 5A top, PLGA-asORN3/1+1 and PLGA-ncasORN).

The time-course of gp*IFNA1* mRNA expression in the asORN3-treated guinea pigs was similar to that of gpIFN-Alpha1 AS. The initial asORN3 inoculation raised the levels of gp*IFNA1* mRNA from 4.9-fold to a more modest 4.0-fold at time points between 24 and 48 h post-infection compared with the negative control animals (Figure 5A bottom, PLGA-asORN3/1 and PLGA-ncasORN). Additional asORN3 inoculation further increased gp*IFNA1* mRNA levels 8.3-fold to 4.8-fold between 24 and 48 h post-infection compared with levels

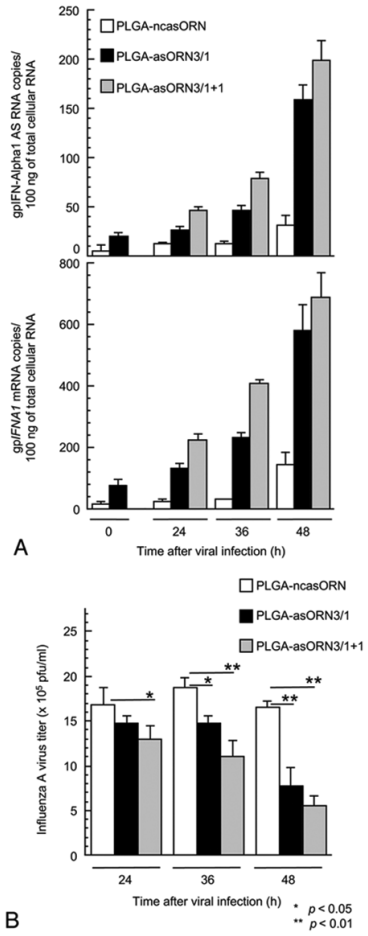

Figure 5. *In vivo* evaluation of asORN3 against respiratory PR/8 virus infection. (A) Effect of nasally administered asORN3 on gpIFN-Alpha1 AS RNA and gp*IFNA1* mRNA expression levels. PLGA-asORN3 (closed bar) or –ncasORN (open bar) was nasally administered to groups of guinea pigs (four animals per group) at -6 hours prior to PR/8 virus infection. Half of the guinea pigs that received PLGA-asORN3 was further administered PLGA-asORN3 (grey bar) at 18 hours after virus infection. The larynx and trachea tissues were collected at various time points ranging from 0 h to 48 h after virus infection. The tissue samples were subsequently subjected to strand-specific RT-qPCR analyses for gpIFN-Alpha1 AS RNA (top) and gp*IFNA1* mRNA (bottom) expression levels. The results are presented as "Mean copy number of gpIFN-Alpha1 AS RNA or mRNA/100 ng of total cellular RNA" ± s.e.m. of four samples. Representative values of three independent experiments are presented. Error bars cannot be seen if they are smaller than the graph symbols. (B) Effect of nasally administered asORN3 on PR/8 virus proliferation profile. PLGA-asORN3 (closed bar or grey bar) or PLGA-ncasORN (open bar) was nasally administered, as described in the Materials and methods. The nasal and tracheal washes were collected at various time points as described in the legend to (A) and were subjected to PR/8 virus titration to monitor the viral proliferation profile in the upper and lower respiratory pathways. The results are presented as "Mean titers ($\times 10^5$ pfu/ml)" ± s.e.m. of four samples. Representative values of three independent experiments are presented.

obtained by ncasORN (Figure 5A bottom, PLGA-asORN3/1+1 and PLGA-ncasORN). These results thus successfully indicated that, as shown for asORN3-transfected 104C1 cells, nasally administered PLGA-asORN3 reproduced the oligoribonucleotide-effects on gpIFN-Alpha1 AS/mRNA expression levels in the respiratory tracts of PR/8 virus-infected guinea pigs.

We then investigated whether or not the increased gp*IFNA1* mRNA levels were capable of reducing PR/8 virus titers in the asORN3-treated animals. Although PR/8 virus infection induced basal levels of gp*IFNA1* mRNA expression in PLGA-ncasORN-treated animals, this level of innate immune response was not enough to limit viral replication in the upper respiratory tract, resulting in increased viral titers in the respiratory washes up to 36 h post-infection (Figure 5B). In contrast, PLGA-asORN3/1 treatment significantly reduced the viral titers in a time-dependent manner by 12% (24 h) to 53% (48 h; $p < 0.01$) at the time points after virus infection indicated within the brackets, respectively.

The additional administration of asORN3 at 18 h post-infection caused further reduction of the viral titers by 23% ($p < 0.05$) at 24 h, 40% ($p < 0.01$) at 36 h, and 67% ($p < 0.01$) at 48 h after virus infection (Figure 5B, PLGA-asORN3/1+1). Neither PR/8 virus infection nor nasal administration of PLGA nanoparticles positively or negatively affected the clinical course of the infection as indicated by comparable levels of both rectal temperature and body weight of animals receiving PLGA-asORNs and virus infection (Figure 6).

5. DISCUSSION

To demonstrate, in a proof-of-concept experiment, that asORNs designed from gpIFN-Alpha1 AS functional domains for gp*IFNA1* mRNA, increase mRNA levels, and thereby, induce anti-viral effects *in vivo*, we developed an animal model system that allowed us to investigate the effects of asORNs on the levels of gpIFN-Alpha1 AS and gp*IFNA1* mRNA in the respiratory tract of PR/8 virus-infected animals.

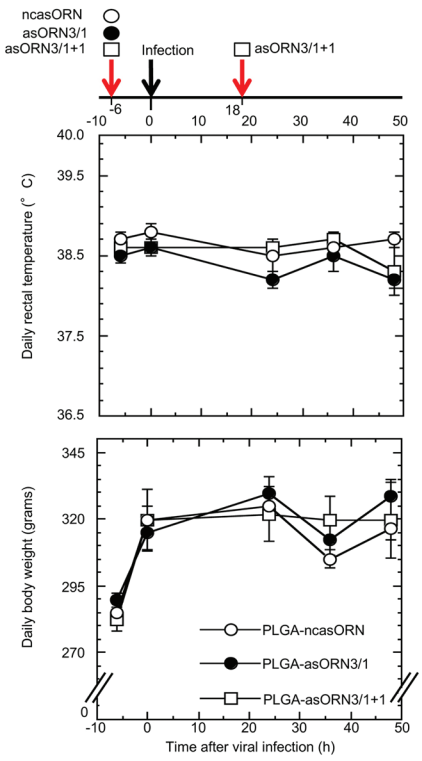

Figure 6. The nasal inoculation of PLGA nanoparticles produced no differences in rectal temperature or body weight between guinea pigs administered asORN3 (closed circle) or ncasORN (open circle) once and guinea pigs administered asORN3 twice (open box). The rectal temperature (top) and body weight (bottom) were monitored at -6 h prior to PR8 virus infection and at 0, 24, 36 and 48 h after the viral infection.

Standard laboratory mouse strains, such as BALB/c and C57BL/6, lack functional *Mx1*, the mouse homolog of human *MX1* (38, 39); therefore, we selected the guinea pig as a model animal, which encodes this important antiviral effector in the type I IFN pathway (21, 29).

In the accompanying study (20) together with our previous report (18), we identified gp*IFNA1* and characterized its anti-viral function. gp*IFNA1* mRNA was expressed with gpIFN-Alpha1 AS in a concordant manner upon PR/8 virus infection in 104C1 cells; therefore, these expression profiles suggested that there is concordant regulation in the expression of gpIFN-Alpha1 AS/mRNA, similar to the observations in *Sendai virus*-infected human Namalwa lymphocytes (18).

We therefore performed an seODN-oriented mapping of the gp*IFNA1* mRNA domains that interact with gpIFN-Alpha1 AS. The subsequent transfection of asORN3/4, representing the gpIFN-Alpha1 AS domains that interact with the mRNA, confirmed *in vitro* their effects on raising the expression levels of gp*IFNA1* mRNA/AS. We then selected PLGA nanoparticles as the drug carrier and determined the optimum packaging conditions of asORN3, which enabled the pulmonary administration of the asORN to the guinea pig model animal. PLGA-asORN3 was then employed to investigate whether the *in vitro* effects of asORNs on the expression levels of gp*IFNA1* mRNA/AS were similar *in vivo*.

Using this experimental strategy, we demonstrated that a functional domain of gpIFN-Alpha1 AS promoted gp*IFNA1* mRNA expression in the respiratory tract of PR/8 virus-infected guinea pigs. This POC experiment thus provided evidence that the natural antisense RNA-mRNA regulatory network we reported previously (16, 18) modulated innate immunity, thereby causing inhibition of PR/8 virus proliferation *in vivo*.

ncRNAs, which do not contain information for the synthesis of specific proteins were predicted in a review in 1965 (40). Today, ncRNAs are gaining increasing recognition because of the development of comprehensive methods that can rapidly analyze entire transcriptomes (10). The lncRNAs are a group of these ncRNAs and 120,353 are currently annotated in the human genome (LNCipedia.org v 5.0.; https://lncipedia.org) (41). Most of them are only predicted by computational analysis, and for the majority of them no function has been attributed. The challenge is, therefore, not only to confirm putative lncRNAs, but also to unveil their functional roles *in vitro* and *in vivo* (42).

We have identified and characterized human IFN-Alpha1 AS, a NAT and a lncRNA, which plays a critical role in the post-transcriptional regulation of *IFNA1*, and subsequently IFN-Alpha protein production (18). A ~ 4 kb,

Table 3. gpasORN3 includes a MRE for mmu-miR-5617-3p

Name	Target sequence[1]
gpasORN3	A U 5' – GAG GUUG AGG **CUGCCUG**–3'
mmu-miR-5617-3p	CUC CGAC UCC **GGCGGAC**–5' 3' –UCA U

[1]The predicted mmu-muR-5617p seed region and the 6-mer MRE site in gpasORN3 are bolded

spliced IFN-Alpha1 AS recognizes a single-stranded region, termed the bulged-stem loop (BSL) within a conserved secondary structure element formed in the *IFNA1* mRNA-coding region. Upon recognition of the BSL region, the cytoplasmic sense-antisense interaction results in stabilization of the *IFNA1* mRNA. This effect was verified by transfection of an asORN, which was designed from the IFN-Alpha 1 AS domain that interacts with the BSL of *IFNA1* mRNA. The asORN raised the levels of *IFNA1* mRNA expression a few fold higher compared with levels in ncasORN-transfected cells, whereas neither the asORN nor ncasORN had any effect on IFN-Alpha1 AS expression (18).

Furthermore, IFN-Alpha1 AS has another synergistic role in the post-transcriptional regulation of human *IFNA1* mRNA stability. IFN-Alpha1 AS shares the MRE-1270s with *IFNA1* mRNA. Interactions between IFN-Alpha1 AS and miR-1270 through the response element titrated away the microRNA from *IFNA1* mRNA, indicating that the AS acts as an endogenous decoy or ceRNA for *IFNA1* mRNA. It followed that an asORN that shares the MRE-1270 sequence, silenced endogenous miR-1270, causing de-repression of not only IFN-Alpha1 AS expression but also *IFNA1* mRNA expression (16).

Similar to the human asORN bearing MRE-1270, guinea pig asORN3 also raised the levels of both gpIFN-Alpha1 AS/mRNA expression, suggesting the possibility that the IFN-Alpha1 AS could promote gp*IFNA1* mRNA expression by inhibiting miR-induced mRNA decay. We, therefore, examined the possibility that asORN3 may act as a decoy to sponge a guinea pig miR (s), leading to the increase of both IFN-Alpha1 AS and mRNA expression levels.

There is no miR database available for *Cavia porcellus*; therefore, we searched for any possible miRs from *Cricetulus griseus*, *Mus musculus* and *Rattus norvegicus* (downloaded from miRBase; http:www.mirbase.org/cgi-bin/browse.pl) that might cross-target asORN3 as a MRE. Following bioinformatic analyses of the miR databases (RegRNA2.0.; http://regrna2.mbe.nctu.edu.tw/; (43), RNA hybrid in BiBiserv; http://bibiserv.techfak.uni-bielefeld.de/rnahybrid/; (44)), the predicted mmu-miR-5617-3p could recognize the asORN3 sequence as a MRE (Table 3).

A subsequent homology search of the guinea pig genome by BLAST (https://www.ensembl.org/index.html) revealed that scaffold_99: 2408710-2408695 and scaffold_25: 9297802-92978171 shared the seed sequence of mmu-miR-56171-3p, which could target the asORN3 sequence region of gpIFN-Alpha1 AS (Table 4) as well as a region of gp*IFNA1* mRNA (Table 5).

asORN3 encodes a probable 6-mer MRE site (45) (see also Table 4); therefore, increased levels of gpIFN-Alpha1 AS and mRNA expression in the asORN3 cells strongly suggested that transfection of asORN3 resulted in potent antagonism of the predicted miRs, leading to the specific de-repression of both gpIFN-Alpha1 AS and gp*IFNA1* mRNA expression.

Furthermore, increased expression levels of gp*IFNA1* mRNA but not gpIFN-Alpha1 AS by asORN4, indicated that gpIFN-Alpha1 AS might raise the levels of gp*IFNA1* mRNA expression by transient duplex formation between the corresponding domain of the AS and the targeted single-stranded region of gp*IFNA1* mRNA in a similar manner to that of human IFN-Alpha1 AS. These findings thus provide the molecular mechanisms of action for guinea pig and human IFN-Alpha1 AS, and indicate the

Table 4. Sequences and locations of target sites matching *Cavia porcellus* homologues of mmu-miR-5617-3p in the guinea pig genome that overlaps *IFNA1* in a reverse orientation

Guinea pig scaffolds	Target sites[1]	Target sequences	Characterization[2]
Scaffold_99: 2408710-2408695 Scaffold_25: 9297802-9297817			
Target miRNA		5'–A A U G–3' GGUUG AGG **CUGCCUG** UCGAC UCC **GGCGGAC**–5' 3' –C	Mfe: -27.0 kcal/mol Nt: 296-313 (asORN3) 6-mer site
Target miRNA		5' –UCU AC C–3' CUGG **CUGCUUG** GACU **GGCGGAC** –5' 3' –CUC CC	Mfe: -16.2 kcal/mol Nt: 346-361 6-mer site
Scaffold_1086: 8283-8269 Scaffold_414: 153840-153826 Scaffold_257: 149027-149013 Scaffold_96: 965907-965921 Scaffold_96: 2849003-2849017 Scaffold_58: 969065-969079 Scaffold_43: 7544061-7544075 Scaffold_14: 25052975-25052989 Scaffold_1: 3700321-3700335			
Target miRNA		5'–A A U G–3' GGUUG AGG **CUGCCUG** 3' – UCGAC UCC **GGCGGAC** –5'	Mfe: -27.0 kcal/mol Nt: 297-313 6-mer site
Target miRNA		5'–CU AC C–3' CUGG **CUGCUUG** GACU **GGCGGAC** –5' 3' –UC CC	Mfe: -16.2 kcal/mol Nt: 347-361 6-mer site
Scaffold_28: 15050517-15050535			
Target miRNA		5' –A UU A U G–3' GAG G G AGG **CUGCCUG** CUC C C UCC **GGCGGAC** –5' 3' – A U GG	Mfe: -29.7 kcal/mol Nt: 294-313 6-mer site

[1]Target: predicted target site including MRE (bolded); miRNA: *Cavia porcellus* homologues of mmu-miR-5617-3p, in which Seed regions are bolded.; [2]Mfe: minimum free energy; Nt: nucleotide number of the target site in gpIFN-Alpha1 AS (nt 564 of *Cavia porcellus IFNA1* was numbered as 1); 6mer-site: type of MRE originally classified by Bartel (45).

possibility that asORNs from the IFN-Alpha1 AS functional domains could be employed for prophylactic and/or therapeutic use to treat the influenza virus infections by modulating *IFNA1* mRNA expression levels, resulting in a type I IFN response against viral infection.

As recently reported by Coch and colleagues (46), type I IFNs are required and sufficient for the treatment of influenza virus infection. The IFNs are expressed and secreted following the detection of viral components within infected cells. Subsequent binding to cognate receptors on cell surfaces leads to the up-regulation of anti-viral genes or IFN-stimulated genes (ISGs). Several ISGs have direct anti-influenza virus activity, including the Mx family of GTPases, which inhibit nuclear

Table 5. Sequences and locations of target sites in the guinea pig *IFNA1* matching *Cavia porcellus* homologues of mmu-miR-5617-3p

Guinea pig scaffolds	Target sites[1]	Target sequences	Characterization[2]
Scaffold_99: 2408710-2408695 Scaffold_25: 9297802-9297817			Mfe: -20.7 kcal/mol Nt: 275-299
Target miRNA		5' –GAUCA GACUCAUCU G–3' GAG **GCUGCCUG** CUC **CGGCGGAC** –5' 3' –CUCGA	Mfe: -20.7 kcal/mol Nt: 275-299 7mer-m8 site
Target miRNA		5' –CACUUUCUC A–3' **CUGCCUG** **GGCGGAC** –5' 3' –CUCGACUCC	Mfe: -16.2 kcal/mol Nt: 144-159 6-mer site
Scaffold_1086: 8283-8269 Scaffold_414: 153840-153826 Scaffold_257: 149027-149013 Scaffold_96: 965907-965921 Scaffold_96: 2849003-2849017 Scaffold_58: 969065-969079 Scaffold_43: 7544061-7544075 Scaffold_14: 25052975-25052989 Scaffold_1: 3700321-3700335			Mfe: -20.7 kcal/mol Nt: 276-299 7mer-m8 site
Target miRNA		5' –GAUCA GACUCAUCU G–3' GAG **GCUGCCUG** CUC **CGGCGGAC** –5' 3' –CUCGA	Mfe: -20.7 kcal/mol Nt: 276-299 7mer-m8 site
Target miRNA		5' –CACUUUCUC A–3' **CUGCCUG** **GGCGGAC** –5' 3' –CUCGACUCC	Mfe: -16.2 kcal/mol Nt: 145-159 6-mer site
Scaffold_28: 15050517-15050535			
Target miRNA		5' –A A CAUCU G–3' GAGG CU **GCUGCCUG** CUCU GG **CGGCGGAC** –5' 3' – A C CUC	Mfe: -24.4 kcal/mol Nt: 279-299 7mer-m8 site
Target miRNA		5' –A AUUU ACUUUCUC A–3' GAGA CC **CUGCCUG** CUCU GG **GGCGGAC** –5' 3' –A C CUCC	Mfe: -20.3 kcal/mol Nt: 134-159 6-mer site
Target miRNA		5' –C CU U G AAUACUUCCACA AUCA A–3' UGA G GC GA GG **CUGUCU** 3' – ACU C CG CU CC **GGCGGA** U G C–5'	Mfe: -15.2 kcal/mol Nt: 422-458 6-mer site

[1]Target: predicted target site including MRE (bolded); miRNA: *Cavia porcellus* homologues of mmu-miR-5617-3p, in which Seed regions are bolded.;.[2]Mfe: minimum free energy; Nt: nucleotide number of the target site in *Cavia porcellus IFNA1;* 7mer-m8 site: type of MRE originally classified by Bartel (45).

import and/or proliferation of viral nucleocapsids, and the IFN-induced trans-membrane (IFITM) family, (especially IFITM3), which interfere with fusion between viral and endosomal membranes, thereby limiting viral entry (for a review see (47) and references therein).

This highlights the fundamental role of IFNs in efficiently limiting further proliferation and spread of the influenza virus. Because inhibition of viral proliferation by type I IFN occurs in infected cells and in surrounding uninfected cells, the induction of IFN-induced anti-viral activities provides a strong rationale for the use of IFN-Alpha1 AS asORNs, not only for prophylaxis, but also to ameliorate the clinical signs of ongoing influenza virus infection by inhibiting both viral entry and viral proliferation.

Our results support, at least in part, the rationale that the initial administration of asORN3 to guinea pigs prior to PR/8 virus infection elevated both IFN-Alpha1 AS and *IFNA1* mRNA expression in the larynx and trachea tissues to higher levels than the control infection even at the time of virus administration and up to 48 h after infection.

The increased RNA levels were associated with significant reductions of viral titers in the upper and lower respiratory tracts in the infected animals up to 48 h after infection. Moreover, the same dose of asORN3 ameliorated the expression of IFN-Alpha1 AS/mRNA and further reduced PR/8 virus titers to a significant degree if administered in the course of the ongoing influenza A virus infection. These results thus indicate that modulation of type I IFN expression could serve as a promising strategy to treat influenza virus infection in both therapeutic and prophylactic settings (48).

In conclusion, we performed a POC experiment to provide evidence that the natural antisense RNA-mRNA regulatory circuitry controls the expression of *IFNA1* mRNA, and subsequently IFN-Alphạproduction, thereby restricting the proliferation of influenza A virus *in vivo*. Optimization of asORN sequences and administration protocols will help the development of new nucleic acid therapeutics for both prevention and treatment of human influenza virus infection.

6. ACKNOWLEDGEMENT

Ryou Sakamoto and Shiwen Jiang contributed equally to this article. The authors declare no competing conflicts of interest with respect to the research, authorship and/or publication of this article. All applicable international, national, and institutional guidelines for the care and use of animals were followed. This article does not contain any studies with human participants performed by any of the authors.We are grateful to Tomoaki Nakano, a former member of the Kimura laboratory, who participated at early stages of the project, Shin-Ichiro Nakamura for providing technical advice for the guinea pig experiments, and to Mikio Nishizawa for critical reading of the manuscript and stimulating discussions. We also thank all the present members of the Kimura laboratory for stimulating discussions. We thank Jeremy Allen, PhD, from Edanz Group (www.edanzediting.com/ac) for editing a draft of this manuscript. This work was supported by Japan Science and Technology Agency (JST) Grant No. AS2511389Q758 and by the Japan Society for the Promotion of Sciences (JSPS) KAKENHI Grant No. 15K06926 to TK.

7. REFERENCES

1. T.R. Mercer, M.E. Dinger, J.S. Mattick: Long non-coding RNAs: insights into functions. *Nat Rev Genet*, 10(3), 155-9 (2009)
DOI: 10.1038/nrg2521
PMid:19188922

2. J. Varilh, J. Bonini, M. Taulan-Cadars: Role of non-coding RNAs in cystic fibrosis. In: *Cystic fibrosis in the light of new research*. Ed D. Wat. InTech, (2015)
DOI: 10.5772/60449

3. R. Bonasio, R. Shiekhattar: Regulation of transcription by long noncoding RNAs.

Annu Rev Genet, 48, 433-55 (2014)
DOI: 10.1146/annurev-genet-120213-092323
PMid:25251851 PMCid:PMC4285387

4. A.A. Sigova, A.C. Mullen, B. Molinie, S. Gupta, D.A. Orlando, M.G. Guenther, A.E. Almada, C. Lin, P.A. Sharp, C. C. Giallourakis, R.A. Young: Divergent transcription of long noncoding RNA/mRNA gene pairs in embryonic stem cells. *Proc Natl Acad Sci U S A*, 110(8), 2876-81 (2013)
DOI: 10.1073/pnas.1221904110
PMid:23382218 PMCid:PMC3581948

5. M. Guttman, I. Amit, M. Garber, C. French, M.F. Lin, D. Feldser, M. Huarte, O. Zuk, B. W. Carey, J.P. Cassady, M.N. Cabili, R. Jaenisch, T.S. Mikkelsen, T. Jacks, N. Hacohen, B.E. Bernstein, M. Kellis, A. Regev, J.L. Rinn, E.S. Lander: Chromatin signature reveals over a thousand highly conserved large non-coding RNAs in mammals. *Nature*, 458(7235), 223-7 (2009)
DOI: 10.1038/nature07672
PMid:19182780 PMCid:PMC2754849

6. I. Ulitsky, A. Shkumatava, C.H. Jan, H. Sive, D.P. BarTel: Conserved function of lincRNAs in vertebrate embryonic development despite rapid sequence evolution. *Cell*, 147(7), 1537-50 (2011)
DOI: 10.1016/j.cell.2011.11.055
PMid:22196729 PMCid:PMC3376356

7. W. Li, D. Notani, M.G. Rosenfeld: Enhancers as non-coding RNA transcription units: recent insights and future perspectives. *Nat Rev Genet*, 17(4), 207-23 (2016)
DOI: 10.1038/nrg.2016.4
PMid:26948815

8. A.C. Seila, J.M. Calabrese, S.S. Levine, G.W. Yeo, P.B. Rahl, R.A. Flynn, R.A. Young, P.A. Sharp: Divergent transcription from active promoters. *Science*, 322(5909), 1849-51 (2008)
DOI: 10.1126/science.1162253
PMid:19056940 PMCid:PMC2692996

9. S. Djebali, C.A. Davis, A. Merkel, A. Dobin, T. Lassmann, A. Mortazavi, A. Tanzer, J. Lagarde, W. Lin, F. Schlesinger, C. Xue, G.K. Marinov, J. Khatun, B.A. Williams, C. Zaleski, J. Rozowsky, M. Roder, F. Kokocinski, R.F. Abdelhamid, T. Alioto, I. Antoshechkin, M.T. Baer, N.S. Bar, P. Batut, K. Bell, I. Bell, S. Chakrabortty, X. Chen, J. Chrast, J. Curado, T. Derrien, J. Drenkow, E. Dumais, J. Dumais, R. Duttagupta, E. Falconnet, M. Fastuca, K. Fejes-Toth, P. Ferreira, S. Foissac, M. J. Fullwood, H. Gao, D. Gonzalez, A. Gordon, H. Gunawardena, C. Howald, S. Jha, R. Johnson, P. Kapranov, B. King, C. Kingswood, O. J. Luo, E. Park, K. Persaud, J. B. Preall, P. Ribeca, B. Risk, D. Robyr, M. Sammeth, L. Schaffer, L.H. See, A. Shahab, J. Skancke, A.M. Suzuki, H. Takahashi, H. Tilgner, D. Trout, N. Walters, H. Wang, J. Wrobel, Y. Yu, X. Ruan, Y. Hayashizaki, J. Harrow, M. Gerstein, T. Hubbard, A. Reymond, S. E. Antonarakis, G. Hannon, M.C. Giddings, Y. Ruan, B. Wold, P. Carninci, R. Guigo, T.R. Gingeras: Landscape of transcription in human cells. *Nature*, 489(7414), 101-8 (2012)
DOI: 10.1038/nature11233
PMid:22955620 PMCid:PMC3684276

10. F. Kopp, J.T. Mendell: Functional Classification and Experimental Dissection of Long Noncoding RNAs. *Cell*, 172(3), 393-407 (2018)
DOI: 10.1016/j.cell.2018.01.011
PMid:29373828

11. M. Nishizawa, Y. Ikeya, T. Okumura, T. Kimura: Post-transcriptional inducible gene regulation by natural antisense RNA. *Front Biosci (Landmark Ed)*, 20, 1-36 (2015)
DOI: 10.2741/4297

12. M. Nishizawa, T. Okumura, Y. Ikeya, T. Kimura: Regulation of inducible gene expression by natural antisense transcripts. *Front Biosci (Landmark Ed)*, 17, 938-58 (2012)
DOI: 10.2741/3965

13. S. Lee, F. Kopp, T.C. Chang, A. Sataluri,

B. Chen, S. Sivakumar, H. Yu, Y. Xie, J.T. Mendell: Noncoding RNA NORAD Regulates Genomic Stability by Sequestering PUMILIO Proteins. *Cell*, 164(1-2), 69-80 (2016)
DOI: 10.1016/j.cell.2015.12.017
PMid:26724866 PMCid:PMC4715682

14. A. Tichon, N. Gil, Y. Lubelsky, T. Havkin Solomon, D. Lemze, S. Itzkovitz, N. Stern-Ginossar, I. Ulitsky: A conserved abundant cytoplasmic long noncoding RNA modulates repression by Pumilio proteins in human cells. *Nat Commun*, 7, 12209 (2016)
DOI: 10.1038/ncomms12209
PMid:27406171 PMCid:PMC4947167

15. Y. Tay, J. Rinn, P.P. Pandolfi: The multilayered complexity of ceRNA crosstalk and competition. *Nature*, 505(7483), 344-52 (2014)
DOI: 10.1038/nature12986
PMid:24429633 PMCid:PMC4113481

16. T. Kimura, S. Jiang, N. Yoshida, R. Sakamoto, M. Nishizawa: Interferon-alpha competing endogenous RNA network antagonizes microRNA-1270. *Cell Mol Life Sci*, 72(14), 2749-61 (2015)
DOI: 10.1007/s00018-015-1875-5
PMid:25746225 PMCid:PMC4477080

17. L. Poliseno, P.P. Pandolfi: PTEN ceRNA networks in human cancer. *Methods*, 77-78, 41-50 (2015)
DOI: 10.1016/j.ymeth.2015.01.013
PMid:25644446

18. T. Kimura, S. Jiang, M. Nishizawa, E. Yoshigai, I. Hashimoto, M. Nishikawa, T. Okumura, H. Yamada: Stabilization of human interferon-alpha1 mRNA by its antisense RNA. *Cell Mol Life Sci*, 70(8), 1451-67 (2013)
DOI: 10.1007/s00018-012-1216-x
PMid:23224365 PMCid:PMC3607724

19. T. Kimura, I. Hashimoto, M. Nishizawa, S. Ito, H. Yamada: Novel cis-active structures in the coding region mediate CRM1-dependent nuclear export of IFN-alpha 1 mRNA. *Med Mol Morphol*, 43(3), 145-57 (2010)
DOI: 10.1007/s00795-010-0492-5
PMid:20857263

20. S. Jiang, R. Sakamoto, T. Kimura: A guinea pig *IFNA1* gene with antiviral activity against human influenza virus infection. *Front Biosci* (In Press)

21. M.A. Horisberger, M. C. Gunst: Interferon-induced proteins: identification of Mx proteins in various mammalian species. *Virology*, 180(1), 185-90 (1991)
DOI: 10.1016/0042-6822(91)90022-4

22. A.C. Lowen, S. Mubareka, J. Steel, P. Palese: Influenza virus transmission is dependent on relative humidity and temperature. *PLoS Pathog*, 3(10), 1470-6 (2007)
DOI: 10.1371/journal.ppat.0030151
PMid:17953482 PMCid:PMC2034399

23. K. Tahara, T. Sakai, H. Yamamoto, H. Takeuchi, N. Hirashima, Y. Kawashima: Improved cellular uptake of chitosan-modified PLGA nanospheres by A549 cells. *Int J Pharm*, 382(1-2), 198-204 (2009)
DOI: 10.1016/j.ijpharm.2009.07.023
PMid:19646519

24. H. Yamamoto, Y. Kuno, S. Sugimoto, H. Takeuchi and Y. Kawashima: Surface-modified PLGA nanosphere with chitosan improved pulmonary delivery of calcitonin by mucoadhesion and opening of the intercellular tight junctions. *J Control Release*, 102(2), 373-81 (2005)
DOI: 10.1016/j.jconrel.2004.10.010
PMid:15653158

25. O. Haller: Inborn resistance of ice to orthomyxoviruses. *Curr Top Microbiol Immunol*, 92, 25-52 (1981)
DOI: 10.1007/978-3-642-68069-4_3
DOI: 10.1007/978-3-642-68069-4
PMid:6171385

26. A. Forsbach, J. G. Nemorin, C. Montino, C. Muller, U. Samulowitz, A.P. Vicari, M. Jurk, G.K. Mutwiri, A.M. Krieg, G.B. Lipford, J. Vollmer: Identification of RNA

sequence motifs stimulating sequence-specific TLR8-dependent immune responses. *J Immunol*, 180(6), 3729-38 (2008)
DOI: 10.4049/jimmunol.180.6.3729
PMid:18322178

27. S. Tluk, M. Jurk, A. Forsbach, R. Weeratna, U. Samulowitz, A. M. Krieg, S. Bauer, J. Vollmer: Sequences derived from self-RNA containing certain natural modifications act as suppressors of RNA-mediated inflammatory immune responses. *Int Immunol*, 21(5), 607-19 (2009)
DOI: 10.1093/intimm/dxp030
PMid:19332442 PMCid:PMC2733840

28. K. Tahara, S. Samura, K. Tsuji, H. Yamamoto, Y. Tsukada, Y. Bando, H. Tsujimoto, R. Morishita, Y. Kawashima: Oral nuclear factor-kappaB decoy oligonucleotides delivery system with chitosan modified poly(D,L-lactide-co-glycolide) nanospheres for inflammatory bowel disease. *Biomaterials*, 32(3), 870-8 (2011)
DOI: 10.1016/j.biomaterials.2010.09.034
PMid:20934748

29. N. Van Hoeven, J.A. Belser, K.J. Szretter, H. Zeng, P. Staeheli, D.E. Swayne, J.M. Katz, T.M. Tumpey: Pathogenesis of 1918 pandemic and H5N1 influenza virus infections in a guinea pig model: antiviral potential of exogenous alpha interferon to reduce virus shedding. *J Virol*, 83(7), 2851-61 (2009)
DOI: 10.1128/JVI.02174-08
PMid:19144714 PMCid:PMC2655560

30. M. Zuker: Mfold web server for nucleic acid folding and hybridization prediction. *Nucleic Acids Res*, 31(13), 3406-15 (2003)
DOI: 10.1093/nar/gkg595
PMid:12824337 PMCid:PMC169194

31. S. Bauer, C. J. Kirschning, H. Hacker, V. Redecke, S. Hausmann, S. Akira, H. Wagner, G.B. Lipford: Human TLR9 confers responsiveness to bacterial DNA via species-specific CpG motif recognition. *Proc Natl Acad Sci U S A*, 98(16), 9237-42 (2001)
DOI: 10.1073/pnas.161293498
PMid:11470918 PMCid:PMC55404

32. K. Takahasi, M. Yoneyama, T. Nishihori, R. Hirai, H. Kumeta, R. Narita, M. Gale, Jr., F. Inagaki, T. Fujita: Nonself RNA-sensing mechanism of RIG-I helicase and activation of antiviral immune responses. *Mol Cell*, 29(4), 428-40 (2008)
DOI: 10.1016/j.molcel.2007.11.028
PMid:18242112

33. C. Zheng, H. Wu: RIG-I “sees” the 5’-triphosphate. *Structure*, 18(8), 894-6 (2010)
DOI: 10.1016/j.str.2010.07.002
PMid:20696389 PMCid:PMC3767985

34. K. Tahara, S. Tadokoro, H. Yamamoto, Y. Kawashima, N. Hirashima: The suppression of IgE-mediated histamine release from mast cells following exocytic exclusion of biodegradable polymeric nanoparticles. *Biomaterials*, 33(1), 343-51 (2012)
DOI: 10.1016/j.biomaterials.2011.09.043
PMid:21993238

35. B.D. Klugherz, P.L. Jones, X. Cui, W. Chen, N.F. Meneveau, S. DeFelice, J. Connolly, R.L. Wilensky, R.J. Levy: Gene delivery from a DNA controlled-release stent in porcine coronary arteries. *Nat Biotechnol*, 18(11), 1181-4 (2000)
DOI: 10.1038/81176
PMid:11062438

36. L.B. Moore, A.J. Sawyer, J. Saucier-Sawyer, W.M. Saltzman, T.R. Kyriakides: Nanoparticle delivery of miR-223 to attenuate macrophage fusion. *Biomaterials*, 89, 127-35 (2016)
DOI: 10.1016/j.biomaterials.2016.02.036
PMid:26967647 PMCid:PMC4924476

37. O. Koenig, D. Zengerle, N. Perle, S. Hossfeld, B. Neumann, A. Behring, M. Avci-Adali, T. Walker, C. Schlensak, H.P. Wendel, A. Nolte: RNA-Eluting Surfaces for the Modulation of Gene Expression as

A Novel Stent Concept. *Pharmaceuticals (Basel)*, 10(1) (2017)
DOI: 10.3390/ph10010023

38. D. Grimm, P. Staeheli, M. Hufbauer, I. Koerner, L. Martinez-Sobrido, A. Solorzano, A. Garcia-Sastre, O. Haller, G. Kochs: Replication fitness determines high virulence of influenza A virus in mice carrying functional Mx1 resistance gene. *Proc Natl Acad Sci U S A*, 104(16), 6806-11 (2007)
DOI: 10.1073/pnas.0701849104
PMid:17426143 PMCid:PMC1871866

39. P. Staeheli, R. Grob, E. Meier, J. G. Sutcliffe, O. Haller: Influenza virus-susceptible mice carry Mx genes with a large deletion or a nonsense mutation. *Mol Cell Biol*, 8(10), 4518-23 (1988)
DOI: 10.1128/MCB.8.10.4518
PMid:2903437 PMCid:PMC365527

40. H. Harris: History: Non-coding RNA foreseen 48 years ago. *Nature*, 497(7448), 188 (2013)
DOI: 10.1038/497188d
PMid:23657339

41. P.J. Volders, K. Verheggen, G. Menschaert, K. Vandepoele, L. Martens, J. Vandesompele, P. Mestdagh: An update on LNCipedia: a database for annotated human lncRNA sequences. *Nucleic Acids Res*, 43(Database issue), D174-80 (2015)
DOI: 10.1093/nar/gku1060
PMid:25378313 PMCid:PMC4383901

42. M. Polovic, S. Dittmar, I. Hennemeier, H. U. Humpf, B. Seliger, P. Fornara, G. Theil, P. Azinovic, A. Nolze, M. Kohn, G. Schwerdt, M. Gekle: Identification of a novel lncRNA induced by the nephrotoxin ochratoxin A and expressed in human renal tumor tissue. *Cell Mol Life Sci* (2017)
PMid:29282485

43. T.H. Chang, H.Y. Huang, J.B. Hsu, S.L. Weng, J.T. Horng, H.D. Huang: An enhanced computational platform for investigating the roles of regulatory RNA and for identifying functional RNA motifs. *BMC Bioinformatics*, 14 Suppl 2, S4 (2013)

44. M. Rehmsmeier, P. Steffen, M. Hochsmann, R. Giegerich: Fast and effective prediction of microRNA/target duplexes. *RNA*, 10(10), 1507-17 (2004)
DOI: 10.1261/rna.5248604
PMid:15383676 PMCid:PMC1370637

45. D.P. Bartel: MicroRNAs: target recognition and regulatory functions. *Cell*, 136(2), 215-33 (2009)
DOI: 10.1016/j.cell.2009.01.002
PMid:19167326 PMCid:PMC3794896

46. C. Coch, J.P. Stumpel, V. Lilien-Waldau, D. Wohlleber, B.M. Kummerer, I. Bekeredjian-Ding, G. Kochs, N. Garbi, S. Herberhold, C. Schuberth-Wagner, J. Ludwig, W. Barchet, M. Schlee, A. Hoerauf, F. Bootz, P. Staeheli, G. Hartmann, E. Hartmann: RIG-I Activation Protects and Rescues from Lethal Influenza Virus Infection and Bacterial Superinfection. *Mol Ther*, 25(9), 2093-2103 (2017)
DOI: 10.1016/j.ymthe.2017.07.003
PMid:28760668 PMCid:PMC5589155

47. M.J. Killip, E. Fodor, R.E. Randall: Influenza virus activation of the interferon system. *Virus Res*, 209, 11-22 (2015)
DOI: 10.1016/j.virusres.2015.02.003
PMid:25678267 PMCid:PMC4638190

48. M. Nishizawa, T. Kimura: RNA networks that regulate mRNA expression and their potential as drug target. *RNA & Disease,* 3, e864 (2016)

Key Words: lncRNA, Interferon, alpha, IFN, Influenza A, Virus, Guinea pig

Send correspondence to: Tominori Kimura, Laboratory of Microbiology and Cell Biology, Department of Pharmacy, College of Pharmaceutical Sciences, Ritsumeikan University, Kusatsu, Shiga 525-8577, Japan, Tel: 81-77-561-2826; Fax: 81-77-561-5203, E-mail: kimurato@ph.ritsumei.ac.jp